G.N.Afanasiev[1], V.G.Kartavenko, J.Ruzicka[2]

TAMM'S PROBLEM IN SCHWINGER'S AND EXACT APPROACHES

_____
[1]E-mail: afanasev@thsun1.jinr.ru
[2]Faculty of Mathematics and Physics, Comenius University,
 84215, Bratislava, Slovakia

1   Introduction

The aim of this consideration is to analyze frequency and angular distributions of the radiation in the so-called Tamm problem. The latter treats the point charge being at rest in medium at the space point $z = -z_0$ up to a moment $t = -t_0$. In the time interval $-t_0 < t < t_0$ the charge moves with the velocity v that can be smaller or greater than the light velocity in medium c_n. After the moment $t = t_0$ the charge is again at rest at the point $z = z_0$. This problem was first considered by Tamm [1] in 1939. Later, it was qualitatively analyzed by Lawson [2,3] and numerically by Zrelov and Ruzicka [4,5]. In 1996, the exact solution of Tamm's problem has been found for the nondispersive medium [6]. A careful analysis of this solution was given in [7]. It was shown there that Tamm's formulae do not describe the Cherenkov radiation (CR) properly.

On the other hand, Schwinger ([8]) suggested to evaluate frequency and angular spectra of the radiation produced by an arbitrarily moving charge without explicit using the electromagnetic field strengths. This method was successfully applied to the consideration of synchrotron motion ([9,10]).

In this consideration, we compare Tamm's and Schwinger's approaches between themselves and with an exact solution of Tamm's problem.

The plan of our exposition is as follows.

In section 2, we reproduce Tamm's frequency and angular distributions of the radiation produced by a point charge moving uniformly on a finite space interval.

In section 3, by applying Schwinger's method to the consideration of Tamm's problem we obtain the instant (i.e., at a given moment of time) angular and frequency distributions of the radiated power. The integration of the angular distribution over time motion gives the angular-frequency distribution of the energy radiated for a finite time interval. Performing angular integration, one gets the frequency distribution of the energy radiated for a finite time interval. In particular cases one arrives either at Tamm-Frank or Tamm formulae.

The exact electromagnetic fields of Tamm' problem are given in Section 4. They are compared with the famous Tamm's formula describing the angular-frequency distribution of the radiated energy. Criteria for the validity of Tamm's formula are given. These criteria are checked by the numerical calculations presented in the same section.

2   Tamm's original approach

Tamm considered the following problem. A point charge is at rest at the point $z = -z_0$ of the z axis up to a moment $t = -t_0$. In the time interval $-t_0 < t < t_0$ it uniformly moves along the z axis with the velocity v greater than the light velocity in medium c_n. For $t > t_0$, the charge is again at rest at the point $z = z_0$. The nonvanishing Fourier component z of the vector potential (VP) is given by

$$A_\omega = \frac{1}{c} \int_{-z_0}^{z_0} \frac{1}{R} j_\omega(x', y', z') \exp(-i\omega R/c_n) dx' dy' dz',$$

where $R = [(x - x')^2 + (y - y')^2 + (z - z')^2]^{1/2}$, $j_\omega = 0$ for $z' < -z_0$ and $z' > z_0$ and $j_\omega = e\delta(x')\delta(y') \exp(-i\omega z'/v)/2\pi$ for $-z_0 < z' < z_0$. Inserting all this into A_ω and

1

integrating over x' and y', one gets

$$A_\omega(x,y,z) = \frac{e}{2\pi c}\int_{-z_0}^{z_0}\frac{dz'}{R}\exp\left[-i\omega(\frac{z'}{v}+\frac{R}{c_n})\right],$$

$$R = [\rho^2 + (z-z')^2]^{1/2}, \quad \rho^2 = x^2 + y^2. \tag{2.1}$$

At large distances from the charge $(R >> z_0)$ one has : $R = R_0 - z'\cos\theta$, $\cos\theta = z/R_0$, $R_0 = (x^2+y^2+z^2)^{1/2}$. Inserting this into (2.1) and integrating over z' one gets

$$A_\omega(\rho,z) = \frac{e\beta q(\omega)}{\pi R_0\omega}\exp\left(-i\omega R_0/c_n\right), \quad q(\omega) = \frac{\sin\left[\omega t_0(1-\beta_n\cos\theta)\right]}{1-\beta_n\cos\theta}, \quad \beta = \frac{v}{c}, \quad \beta_n = \frac{v}{c_n}. \tag{2.2}$$

Now we evaluate the field strengths. In the wave zone, where $R_0 >> c/n\omega$, the nonvanishing spherical components are

$$E_\theta = H_\phi = -\frac{2e\beta}{\pi cR_0}\sin\theta\int_0^\infty nq(\omega)\sin[\omega(t-R_0/c_n)]d\omega. \tag{2.3}$$

The energy flux through the sphere of the radius R_0 is

$$W = R_0^2\int S_r\sin\theta d\theta d\phi, \quad S_r = \frac{c}{4\pi}E_\theta H_\phi.$$

Inserting E_θ and H_ϕ one obtains

$$W = \frac{2e^2\beta^2}{\pi c}\int_0^\infty nJ(\omega)d\omega, \quad J(\omega) = \int_0^\pi q^2\sin\theta d\theta. \tag{2.4}$$

For $\omega t_0 >> 1$, J can be evaluated in a closed form

$$J = J_{BS} = \frac{1}{\beta^3 n^3}(\ln\frac{1+\beta_n}{|1-\beta_n|} - 2\beta_n) \quad \text{for} \quad \beta_n < 1 \quad \text{and} \tag{2.5}$$

$$J = J_{BS} + J_{Ch}, \quad J_{Ch} = \frac{\pi\omega t_0}{\beta_n}(1-\frac{1}{\beta_n^2}) \quad \text{for} \quad \beta_n > 1. \tag{2.6}$$

Tamm identified J_{BS} with the spectral distribution of the bremsstrahlung BS , arising from instant acceleration and deceleration of the charge at the moments $\pm t_0$, resp. On the other hand, J_{Ch} was identified with the spectral distribution of the Cherenkov radiation. This is supported by the fact that

$$W_{Ch} = \frac{2e^2\beta^2}{\pi c}\int_0^\infty nJ_{Ch}(\omega)d\omega = \frac{2e^2\beta t_0}{c}\int_{\beta_n>1}\omega d\omega(1-\frac{1}{\beta_n^2}). \tag{2.7}$$

strongly resembles the famous Frank-Tamm formula [11] for an infinite medium obtained in quite a different way.

The main result following from Tamm's formulae is that the energy emitted during the whole charge motion into the solid angle $d\Omega$, in the frequency interval $d\omega$ is given by

$$\frac{d^2\mathcal{E}}{d\Omega d\omega} = \frac{e^2}{\pi^2 cn}[\sin\theta\frac{\sin\omega t_0(1-\beta_n\cos\theta)}{\cos\theta - 1/\beta_n}]^2. \tag{2.8}$$

This formula is frequently used by experimentalists (see, e.g., [12-14]) for the identification of Cherenkov radiation.

2

3 Schwinger's approach to Tamm's problem

We begin with the continuity equation following from Maxwell equations

$$div\vec{S} + \frac{\partial}{\partial t}\mathcal{E} = -\vec{j}\vec{E}. \tag{3.1}$$

Here

$$\vec{S} = \frac{c}{4\pi}(\vec{E} \times \vec{H}), \quad \mathcal{E} = \frac{1}{8\pi}(\epsilon E^2 + \mu H^2).$$

Integrating this equation over the volume V of sphere S of the radius r surrounding a moving charge, one gets the following equation describing the energy conservation

$$\int S_r r^2 d\Omega + \frac{\partial}{\partial t}\int \mathcal{E}dV = -\int \vec{j}\vec{E}dV. \tag{3.2}$$

Usual interpretation of this equation proceeds as follows (see, e.g., [15], pp.276-277):
    "The first term on the left-hand side represents the electromagnetic energy flowing out of the volume V through the surface S_r, and the second term represents the time rate of change of the energy stored by the electromagnetic field within V". And further: "The right-hand side, on the other hand, represents the power supplied by the external forces that maintain the charges in dynamic equilibrium."
    Schwinger ([8]) identifies energy losses of a moving charge with the integral in the r.h.s. of (3.1)

$$W_S = -\int \vec{j}\vec{E}dV. \tag{3.3}$$

Substituting $\vec{E} = -\nabla\Phi - \dot{\vec{A}}/c$ and integrating by parts, one gets

$$W_S = -\int \vec{j}\vec{E}dV = \int \vec{j}(\nabla\Phi + \dot{\vec{A}}/c)dV = -\int (div\vec{j} - \dot{\vec{A}}/c)dV = \int (\dot{\rho}\Phi + \dot{\vec{A}}/c)dV =$$

$$= \frac{d}{dt}\int \rho\Phi dV - \int (\rho\dot{\Phi} - \dot{\vec{A}}/c)dV. \tag{3.4}$$

By definition, W_S is the energy lost by a moving charge per unit time.
Schwinger discards the first term in the second line of (3.4) on the grounds that "it is of an accelerated energy type".
The retarded and advanced electromagnetic potentials corresponding to charge current densities ρ and $\vec{j}$ are given by

$$\Phi_{ret,adv} = \frac{1}{\epsilon}\int \frac{1}{R}\rho(\vec{r'},t')\delta(t'-t\pm R/c_n)dV'dt' =$$

$$= \frac{1}{2\pi\epsilon}\int\limits_{-\infty}^{\infty} d\omega \frac{1}{R}\rho(\vec{r'},t')\exp[i\omega(t'-t\pm R/c_n)]dV'dt',$$

$$\vec{A}_{ret,adv} = \frac{\mu}{c}\int \frac{1}{R}\vec{j}(\vec{r'},t')\delta(t'-t\pm R/c_n)dV'dt' =$$

3

$$\frac{\mu}{2\pi c} \int\limits_{-\infty}^{\infty} d\omega \frac{1}{R}\vec{j}(\vec{r}',t') \exp[i\omega(t'-t\pm R/c_n)]d\omega dV'dt', \qquad (3.5)$$

where ϵ and μ are the electric and magnetic permittivities,resp.; $R = |\vec{r}-\vec{r}'|$ and $+$ and $-$ signs refer to retarded and advanced potentials, resp.

Further, Schwinger represents retarded electromagnetic potentials in the form

$$\Phi_{ret} = \frac{1}{2}(\Phi_{ret} + \Phi_{adv}) + \frac{1}{2}(\Phi_{ret} - \Phi_{adv}),$$

$$\vec{A}_{ret} = \frac{1}{2}(\vec{A}_{ret} + \vec{A}_{adv}) + \frac{1}{2}(\vec{A}_{ret} - \vec{A}_{adv}) \qquad (3.6)$$

and discards the symmetric part of these equations on the grounds that "the first part of (3.3), derived from the symmetrical combination of $\vec{E}_{ret}$ and $\vec{E}_{adv}$, changes sign on reversing the positive sense of time and therefore represents reactive power. It describes the rate at which the electron stores energy in the electromagnetic field, an inertial effect with which we are not concerned. However, the second part of (3.3), derived from the antisymmetrical combination of $\vec{E}_{ret}$ and $\vec{E}_{adv}$, remains unchanged on reversing the positive sense of time and therefore represents resistive power. Subject to one qualification, it describes the rate of irreversible energy transfer to the electromagnetic field, which is the desired rate of radiation".

Correspondingly, electromagnetic potentials are reduced to

$$\Phi = -\frac{1}{\pi\epsilon} \int\limits_{0}^{\infty} d\omega \frac{1}{R}\rho(\vec{r}',t') \sin[\omega(t'-t)]\sin(k_n R)dV'dt',$$

$$\vec{A} = -\frac{\mu}{\pi c} \int\limits_{0}^{\infty} d\omega \frac{1}{R}\vec{j}(\vec{r}',t') \sin[\omega(t'-t)]\sin(k_n R/)dV'dt', \quad k_n = \omega/c_n. \qquad (3.7)$$

Substituting this into (3.4), we get

$$W_S = \int\limits_{0}^{\infty} P(\omega,t)d\omega, \qquad (3.8)$$

where

$$P(\omega,t) = \frac{d^2 E}{dt d\omega} = -\frac{\omega}{\pi\epsilon} \int dV\,dV'dt' \frac{\sin k_n R}{R} \cos\omega(t-t')\times$$

$$\times[\rho(\vec{r},t)\rho(\vec{r}',t') - \frac{1}{c_n^2}\vec{j}(\vec{r},t)\vec{j}(\vec{r}',t')] \qquad (3.9)$$

is the energy lost by a moving charge per unit time and per frequency unit. The angular distribution $P(\vec{n},\omega,t)$ is defined as

$$P(\omega,t) = \int P(\vec{n},\omega,t)d\Omega, \qquad (3.10)$$

where

$$P(\vec{n},\omega,t) = \frac{d^3 E}{dt d\omega d\Omega} = -\frac{n\omega^2}{4\pi^2 c\epsilon} \int dV\,dV'dt' \cos\omega[(t'-t) + \frac{1}{c_n}\vec{n}(\vec{r}-\vec{r}')]\times$$

4

$$\times[\rho(\vec{r},t)\rho(\vec{r}',t') - \frac{1}{c_n^2}\vec{j}(\vec{r},t)\vec{j}(\vec{r}',t')] \tag{3.11}$$

is the energy lost by a moving charge per unit time, per frequency unit, and per unit solid angle. Here $\vec{n}$ is the vector defining the observation point.

In what follows we limit ourselves to dielectric medium for which $\epsilon = n^2$.

3.1   Instant power frequency spectrum

For the treated Tamm problem, charge and current densities are given by

$$j_z = ev\delta(x)\delta(y)\Theta(t+t_0)\Theta(t_0-t)\delta(z-vt), \quad \rho(\vec{r},t) = e\delta(x)\delta(y)\times$$

$$\times[\Theta(-t-t_0)\delta(z+z_0) + \Theta(t+t_0)\Theta(t_0-t)\delta(z-vt) + \Theta(t-t_0)\delta(z-z_0)]. \tag{3.12}$$

Inserting these expressions into (3.9) and performing integrations, one gets

$$P(\omega,t) = -\frac{\omega e^2}{\pi\epsilon}[\Theta(-t-t_0)P_1 + \Theta(t-t_0)P_2 + \Theta(t+t_0)\Theta(t_0-t)P_3], \tag{3.13}$$

where

$$P_1 = -\frac{\sin\omega(t+t_0)}{c_n} + \frac{\sin 2\omega t_0\beta_n}{2\omega t_0 v}\sin\omega(t-t_0)+$$

$$+\frac{1}{2v}\cos\omega(t+t_0)\{si[2t_0\omega(1+\beta_n)] - si[2t_0\omega(1-\beta_n)]\}+$$

$$+\frac{1}{2v}\sin\omega(t+t_0)\{\frac{1}{2}\ln(\frac{1+\beta_n}{1-\beta_n})^2 + ci[2\omega t_0|1-\beta_n|] - ci[2\omega t_0(1+\beta_n)]\},$$

$$P_2 = \frac{\sin\omega(t-t_0)}{c_n} - \frac{\sin 2\omega t_0\beta_n}{2vt_0\omega}\sin\omega(t+t_0)+$$

$$+\frac{1}{2v}\cos\omega(t-t_0)\{si[2t_0\omega(1+\beta_n)] - si[2t_0\omega(1-\beta_n)]\}-$$

$$-\frac{1}{2v}\sin\omega(t-t_0)\{\frac{1}{2}\ln(\frac{1+\beta_n}{1-\beta_n})^2 + ci[2\omega t_0|1-\beta_n|] - ci[2\omega t_0(1+\beta_n)]\},$$

$$P_3 = -\frac{\sin\omega\beta_n(t+t_0)}{v(t+t_0)}\frac{\sin\omega(t+t_0)}{\omega} + \frac{\sin\omega\beta_n(t-t_0)}{v(t-t_0)}\frac{\sin\omega(t-t_0)}{\omega} - \frac{1-\beta_n^2}{2v}\times$$

$$\times\{si[(1-\beta_n)\omega(t_0-t)] - si[(1+\beta_n)\omega(t_0-t)] + si[(1-\beta_n)\omega(t_0+t)] - si[(1+\beta_n)\omega(t_0+t)]\}. \tag{3.14}$$

Here $si(x)$ and $ci(x)$ are the integral sine and cosine. They are defined by the equations

$$si(x) = -\int_x^\infty \frac{\sin t}{t}dt = -\frac{\pi}{2} + \int_0^x \frac{\sin t}{t}dt = -\frac{\pi}{2} - \sum_{k=1}^\infty \frac{(-1)^k}{(2k-1)(2k-1)!}x^{2k-1},$$

$$ci(x) = -\int_x^\infty \frac{\cos t}{t}dt = C + \ln x - \int_0^x \frac{1-\cos t}{t}dt = C + \ln x + \sum_{k=1}^\infty \frac{(-1)^k}{2k)(2k)!}x^{2k}.$$

Here $C \approx 0.577$ is Euler's constant. For large and small x, $si(x)$ and $ci(x)$ behave as

$$si(x) \to -\frac{\cos x}{x}, \quad ci(x) \to \frac{\sin x}{x} \quad \text{for} \quad x \to +\infty,$$

5

$$si(x) \to -\pi + \frac{\cos x}{|x|} \quad \text{for} \quad x \to -\infty,$$

$$si(x) \to -\frac{\pi}{2} + x, \quad ci(x) \to C + \ln x - \frac{x^2}{4} \quad \text{for} \quad x \to 0.$$

The following relations

$$\int_0^x \frac{\sin^2 t}{t} dt = \frac{1}{2}C + \frac{1}{2}\ln 2|x| - \frac{1}{2}ci(2|x|), \quad si(x) + si(-x) = -\pi$$

will be also useful.

The nonvanishing of P_1 and P_2 terms in (3.13) is due to the fact that Fourier transforms of a static charge density corresponding to charge at rest prior to the beginning of the charge motion $(t < -t_0)$ and after its termination $(t > t_0)$ contribute to (3.9) and (3.11). To see this explicitly, we write out the Fourier transform of charge density (3.12):

$$\rho(\vec{r}, \omega) = \frac{1}{2\pi} \int_{-\infty}^{\infty} \exp(-i\omega t)\rho(\vec{r}, t)dt =$$

$$= \frac{1}{2\pi}e\delta(x)\delta(y)[\delta(z+z_0)\int_{-\infty}^{-t_0} \exp(-i\omega t)dt + \delta(z-z_0)\int_{t_0}^{\infty} \exp(-i\omega t)dt + \frac{1}{v}\exp(-i\omega z/v)].$$

The first term in the r.h.s. corresponds to the charge which rests at the point $z = -z_0$ up to a moment $t = -t_0$; the second term in the r.h.s. corresponds to the charge which rests at the point $z = z_0$ after the moment $t = t_0$. Finally, third term corresponds to the charge moving between $-z_0$ and z_0 points in the time interval $-t_0 < t < t_0$. It should be noted that first and second terms in this expression are Fourier densities of a charge which does not permanently rest at $z = \pm z_0$ points, but up to a moment $-t_0$ and after the moment t_0, resp. In fact, the Fourier density corresponding to charge which permanently is at rest at the point $z = z_0$ is

$$\frac{e}{2\pi}\delta(z-z_0)\int_{-\infty}^{\infty} \exp(i\omega t)dt = e\delta(z-z_0)\delta(\omega).$$

In the limit $\omega t_0 \to \infty$, Eqs. (3.14) pass into

$$P_1 = -\frac{1}{c_n}\sin[\omega(t+t_0)](1 - \frac{1}{2\beta_n}\ln\frac{1+\beta_n}{1-\beta_n}),$$

$$P_2 = +\frac{1}{c_n}\sin[\omega(t-t_0)](1 - \frac{1}{2\beta_n}\ln\frac{1+\beta_n}{1-\beta_n}), \quad P_3 = 0$$

for $\beta_n < 1$ and

$$P_1 = -\frac{1}{c_n}\sin[\omega(t+t_0)](1 - \frac{1}{2\beta_n}\ln\frac{1+\beta_n}{\beta_n - 1}) + \frac{\pi}{2v}\cos\omega(t + \frac{z_0}{v}),$$

$$P_2 = \frac{1}{c_n}\sin[\omega(t-t_0)](1 - \frac{1}{2\beta_n}\ln\frac{1+\beta_n}{\beta_n - 1}) + \frac{\pi}{2v}\cos\omega(t - \frac{z_0}{v}), \quad P_3 = -\frac{\pi}{v}(\beta_n^2 - 1) \quad (3.15)$$

6

for $\beta_n > 1$. It is seen that the energy radiated for the time interval $-t_1 < t < t_1$, $t_1 \ll t_0$ equals zero for $\beta_n < 1$ and equals $\omega e^2 t_1 (\beta_n^2 - 1)/\pi v$ for $\beta_n > 1$. This exactly coincides with the Cherenkov radiation spectrum for unbounded charge motion (see, e.g., Frank's book [11]). It should be noted that expressions for P_3 in (3.15) were obtained under the assumption that arguments of si and ci of P_3 entering into (3.14) are sufficiently large, that is, there should be $\omega(t_0 - t) >> 1$. This means that P_3 in (3.15) are valid if t is not too close to t_0.

On the other hand, terms P_1 and P_2 in (3.15) were obtained without this assumption. In particular, the term P_2 different from zero for $t > t_0$ shows how the bremsstralung (BS) and Cherenkov radiation behave for $t > t_0$, i.e., after termination of charge motion. Since the part of P_2

$$\frac{1}{c_n} \sin \omega(t - \frac{z_0}{v})(1 - \frac{1}{2\beta_n} \ln \frac{\beta_n + 1}{|\beta_n - 1|})$$

is present both for $\beta_n < 1$ and $\beta_n > 1$, it may be associated with BS. On the other hand, the part of P_2

$$\frac{\pi}{2v} \cos[\omega(t - \frac{z_0}{v})]$$

that differs from zero only for $\beta_n > 1$ may be conditionally attributed to the Cherenkov post-action.

We observe that for $t < -t_0$ and $t > t_0$, the radiation intensity is a rapidly oscillating function of time t. Time average of this intensity is zero, so it could hardly be observed experimentally. Since, on the other hand, for $\beta_n > 1$, the radiation intensity does not depend on time in the time interval $-t_1 < t < t_1$, $t_1 << t_0$, it contributes coherently to the radiated energy.

To obtain the energy radiated for a finite time interval, one should integrate (3.13) over t. However, the arising integrals involve integral sine and cosine functions. Since we did not succeed to evaluate these integrals in a closed form, we follow an indirect way in next sections. In section 3.2, we evaluate the instant angular-frequency distribution of the radiated energy. Integrating it over time we obtain (Sect. 3.3) the angular-frequency distribution of the energy radiated for a finite time interval. Finally, integrating latter over angular variables we obtain a closed expression for the frequency distribution of the energy radiated for a finite time interval (Sect. 3.4).

3.2   Instant angular-frequency distribution of power spectrum

Due to the axial symmetry of the problem, $\vec{n}(\vec{r} - \vec{r}') = \cos\theta(z - z')$ in the integrand in (3.11), where θ is the inclination angle of $\vec{n}$ towards the motion axis. Integration over space-time variables in (3.11) gives

$$P(\vec{n}, \omega, t) = \frac{d^3 \mathcal{E}}{dt d\omega d\Omega} = -\frac{\omega e^2 \beta}{2\pi^2 c} \frac{\sin[\omega t_0 (1 - \beta_n \cos\theta)]}{1 - \beta_n \cos\theta} \times$$

$$\times [\Theta(-t - t_0)P_{1n} + \Theta(t - t_0)P_{2n} + \Theta(t + t_0)\Theta(t_0 - t)P_{3n}]. \qquad (3.16)$$

Here

$$P_{1n} = \cos\theta \cos[\omega(t + t_0\beta_n \cos\theta)], \qquad P_{2n} = \cos\theta \cos[\omega(t - t_0\beta_n \cos\theta)],$$

$$P_{3n} = (\cos\theta - \beta_n) \cos[\omega t(1 - \beta_n \cos\theta)].$$

In what follows we limit ourselves to dielectric medium for which $\epsilon = n^2$.

3.3 Angular-frequency distibution of the radiated energy for a finite time interval

Integrating (3.16) over the time interval $-t_1 < t < t_1,\quad t_1 < t_0$, one obtains the Fourier distribution of the energy detected for a time $2t_1$ radiated by a particle moving in the time interval $2t_0,\quad t_1 < t_0$:

$$\mathcal{E}(\vec{n},\omega,t_1) = \int_{-t_1}^{t_1} P(\vec{n},\omega,t)dt = \frac{e^2\beta}{\pi^2 c}(\beta_n - \cos\theta)\frac{\sin\omega t_0(1-\beta_n\cos\theta)}{1-\beta_n\cos\theta}\frac{\sin\omega t_1(1-\beta_n\cos\theta)}{1-\beta_n\cos\theta}.$$

$$(3.17)$$

Let $\omega t_0 \to \infty$. Then,

$$\mathcal{E}(\vec{n},\omega,t_1) \to \frac{e^2\beta\omega t_1}{\pi c}(1-\frac{1}{\beta_n^2})\delta(\cos\theta - \frac{1}{\beta_n}).$$

$$(3.18)$$

This coincides with the angular-frequency distribution of the radiated energy in Tamm-Frank theory [11] describing the unbounded charge motion. For $\cos\theta = 1/\beta_n$ Eq. (3.17) reduces to

$$\mathcal{E}(\vec{n},\omega,t_1) = \frac{e^2}{\pi n c}(\beta_n^2-1)\omega^2 t_0 t_1.$$

It vanishes for $\beta_n = 1$.

Let $t_1 > t_0$. Then,

$$\mathcal{E}(\vec{n},\omega,t_1) = \frac{e^2\beta}{\pi^2 c}\frac{\sin[\omega t_0(1-\beta_n\cos\theta)]}{1-\beta_n\cos\theta}\times$$

$$[\beta_n\sin^2\theta\frac{\sin\omega t_0(1-\beta_n\cos\theta)}{1-\beta_n\cos\theta} - \cos\theta\sin\omega(t_1-t_0\beta_n\cos\theta)]\qquad(3.19)$$

is the angular-frequency distribution of the energy detected for the time inerval $2t_1 > 2t_0$. The first term in square brackets coincides with Tamm's angular distribution (2.8). The second term originating from integration of P_1 and P_2 terms in (3.16) describes the boundary effects. The physical reason for the appearance of the extra term in (3.19)(second term in square brackets) is due to the following reason. The magnetic field $\vec{H}$ is defined as *curl* of VP (2.2). Tamm obtained electric field from the Maxwell equation

$$curl\vec{H} = \frac{\epsilon}{c}\frac{\partial\vec{E}}{\partial t}$$

valid outside the motion interval. In the ω representation this equation looks as

$$curl\vec{H}_\omega = \frac{i\omega\epsilon}{c}\vec{E}_\omega.$$

This equation suggests that contribution of static electric field existing before beginning of charge motion and after its termination has dropped from Tamm's formulae given in section 2.

As we have seen earlier, Schwinger's equations (3.9) and (3.11) contain the static electric field contributions of a charge which is at rest up to the moment $t = -t_0$ and after the

8

moment $t = t_0$. They are responsible for the appearance of extra term in (3.19). In the $\vec{r}, t$ representation, the contribution of the static electromagnetic field strengths is not essential in the wave zone.

Taking into account that

$$\frac{\sin \alpha x}{x} \to \pi \delta(x) \quad \text{and} \quad \frac{1}{\alpha}[\frac{\sin \alpha x}{x}]^2 \to \pi \delta(x) \quad \text{for} \quad \alpha \to \infty, \tag{3.20}$$

one obtains from (3.19) for large ωt_0

$$\mathcal{E}(\vec{n}, \omega, t_1) = \frac{e^2}{\pi c n} \delta(1 - \beta_n \cos \theta)[\omega t_0(\beta_n^2 - 1) - \sin \omega(t_1 - \frac{z_0}{v})]. \tag{3.21}$$

For $\beta_n \neq 1$, the second term inside the square brackets may be discarded, and one gets

$$\mathcal{E}(\vec{n}, \omega, t_1) = \frac{e^2}{\pi c n} \omega t_0(\beta_n^2 - 1) \delta(1 - \beta_n \cos \theta). \tag{3.22}$$

For $\cos \theta = 1/\beta_n$, Eq. (3.19) is reduced to

$$\mathcal{E}(\vec{n}, \omega, t_1) = \frac{e^2}{\pi n c}(\beta_n^2 - 1)\omega^2 t_0^2 - \frac{e^2}{\pi n c} \omega t_0 \sin \omega(t_1 - t_0).$$

It does not vanish at $\beta_n = 1$.

Equations (3.17) and (3.19) are generalizations of Tamm's angular-frequency distributions for $t_1 \neq t_0$.

3.4 Frequency distribution of the radiated energy

Integrating (3.17) over the solid angle one, finds the following expression for the frequency distribution of the radiated power for the case when the detection time $2t_1$ is smaller than the motion time $2t_0$:

$$\mathcal{E}(\omega, t_1) = \frac{e^2 \beta_n}{\pi c n}(1 - \frac{1}{\beta_n^2})\{\frac{\cos(\omega(t_1 - t_0)(1 - \beta_n))}{1 - \beta_n} - \frac{\cos(\omega(t_0 - t_1)(1 + \beta_n))}{1 + \beta_n}$$

$$-\frac{\cos(\omega(t_1 + t_0)(1 - \beta_n))}{1 - \beta_n} + \frac{\cos(\omega(t_1 + t_0)(1 + \beta_n))}{1 + \beta_n} +$$

$$+\omega(t_0 - t_1)[si(\omega(t_0 - t_1)(1 - \beta_n)) - si(\omega(t_0 - t_1)(1 + \beta_n))]$$

$$-\omega(t_0 + t_1)[si(\omega(t_0 + t_1)(1 - \beta_n)) - si(\omega(t_0 + t_1)(1 + \beta_n))]\}$$

$$-\frac{e^2}{\pi \epsilon v}[ci(\omega(t_0 - t_1)|1 - \beta_n|) - ci(\omega(t_0 - t_1)(1 + \beta_n))$$

$$-ci(\omega(t_0 + t_1)|1 - \beta_n|) + ci(\omega(t_0 + t_1)(1 + \beta_n))]. \tag{3.23}$$

Now let $t_1 > t_0$ (i.e., the detection time is greater than the motion time). Then,

$$\mathcal{E}(\omega, t_1) = \frac{2e^2 \beta_n}{\pi c n}(\beta_n I_1 - I_2), \tag{3.24}$$

where

$$I_1 = \int \sin^3 \theta d\theta [\frac{\sin \omega t_0(1 - \beta_n \cos \theta)}{1 - \beta_n \cos \theta}]^2 = \frac{1}{\beta_n}(1 - \frac{1}{\beta_n^2}) \times$$

9

$$\times\{\frac{\sin^2\omega t_0(1-\beta_n)}{1-\beta_n} - \frac{\sin^2\omega t_0(1+\beta_n)}{1+\beta_n} - \omega t_0[si(2\omega t_0(1-\beta_n)) - si(2\omega t_0(1+\beta_n))]\} -$$

$$-\frac{1}{\beta_n^3}[\ln\frac{|1-\beta_n|}{1+\beta_n} - ci(2\omega t_0|1-\beta_n|) + ci(2\omega t_0(1+\beta_n))] -$$

$$-\frac{1}{\beta_n^2} - \frac{1}{4\beta_n^3\omega t_0}[\sin(2\omega t_0(1-\beta_n)) - \sin(2\omega t_0(1+\beta_n))],$$

$$I_2 = \int \sin\theta\cos\theta d\theta \frac{\sin\omega t_0(1-\beta_n\cos\theta)\sin\omega(t_1-t_0\beta_n\cos\theta)}{1-\beta_n\cos\theta} =$$

$$= -\frac{1}{4\beta_n^2\omega t_0}\sin\omega(t_1-t_0)[\cos(2\omega t_0(1-\beta_n)) - \cos(2\omega t_0(1+\beta_n))] -$$

$$-\frac{1}{\beta_n}\cos\omega(t_1-t_0) - \frac{1}{4\beta_n^2\omega t_0}\cos\omega(t_1-t_0)[\sin(2\omega t_0(1-\beta_n)) - \sin(2\omega t_0(1+\beta_n))] -$$

$$-\frac{1}{2\beta_n^2}\sin\omega(t_1-t_0)[si(2\omega t_0(1-\beta_n)) - si(2\omega t_0(1+\beta_n))] -$$

$$\frac{1}{2\beta_n^2}\cos\omega(t_1-t_0)[\ln\frac{|1-\beta_n|}{1+\beta_n} - ci(2\omega t_0|1-\beta_n|) + ci(2\omega t_0(1+\beta_n))].$$

The typical dependence of $\mathcal{E}$ on t_0 for t_1 fixed is shown in Fig.1. For $\beta_n < 1$, it oscillates around the zero value. The amplitude of oscillations decreases like $1/\omega t_0$ for large t_0. For $\beta_n > 1$, $\mathcal{E}$ oscillates around the value

$$\frac{2e^2\omega t_1\beta}{c}(1 - \frac{1}{\beta_n^2}),$$

given by the Tamm-Frank theory [11].
The typical dependence of $\mathcal{E}$ on t_1 for t_0 fixed is shown in Fig.2. For $\beta_n < 1$ and $\beta_n > 1$, it oscillates around the values

$$\frac{4e^2}{\pi cn}(\frac{1}{2\beta_n}\ln\frac{1+\beta_n}{1-\beta_n} - 1) \quad \text{and}$$

$$\frac{2e^2\beta}{c}\omega t_0(1 - \frac{1}{\beta_n^2}) + \frac{4e^2}{\pi cn}(\frac{1}{2\beta_n}\ln\frac{1+\beta_n}{\beta_n - 1} - 1)], \quad \text{resp.}$$

predicted by the Tamm theory (see Eqs.(2.5) and (2.6)).
Previously, the frequency distribution of the radiated energy in the framework of Tamm's theory was given by Kobzev and Frank [16]. It was obtained by integrating (2.8) over the angular variables:

$$\frac{d\mathcal{E}}{d\omega} = \frac{2e^2\beta}{\pi c}(1 - \frac{1}{\beta_n^2})\{\frac{\sin^2\omega t_0(1-\beta_n)}{1-\beta_n} - \frac{\sin^2\omega t_0(1+\beta_n)}{1+\beta_n}$$

$$-\omega t_0[si(2\omega t_0(1-\beta_n)) - si(2\omega t_0(1+\beta_n))]\} -$$

$$-\frac{2e^2}{\pi cn\beta_n}[\ln\frac{|1-\beta_n|}{1+\beta_n} - ci(2\omega t_0|1-\beta_n|) + ci(2\omega t_0(1+\beta_n))] -$$

$$-\frac{e^2}{\pi c n \beta_n}\{2\beta_n + \frac{1}{2\omega t_0}[\sin 2\omega t_0(1-\beta_n)) - \sin 2\omega t_0(1+\beta_n))]\}. \qquad (3.25)$$

For large ωt_0 one gets Tamm's equations (2.5) and (2.6).

The frequency dependences of the energy radiated for the time t_1 are shown in Figs. 3 and 4. In Fig. 3, one sees the frequency dependence for the case when the observation time $2t_1$ is twice as small as the charge motion time $2t_0$. For $\beta_n < 1$, the radiated energy is concentrated near zero, while for $\beta_n > 1$ it rises linearly with frequency

$$\mathcal{E} \sim \frac{2e^2\omega t_1 \beta_n}{cn}(1 - \frac{1}{\beta_n^2}).$$

The frequency dependence for the case when the observation time $2t_1$ is twice as the charge motion time $2t_0$ is shown in Fig. 4. For $\beta_n < 1$, the radiated energy oscillates around Tamm's value

$$\frac{4e^2}{\pi cn}(\ln \frac{1+\beta_n}{1-\beta_n} - 1),$$

while for $\beta_n > 1$, it again rises linearly but with a coefficient different from the previous case:

$$\mathcal{E} \sim \frac{2e^2\omega t_0 \beta}{c}(1 - \frac{1}{\beta_n^2}).$$

3.4.1 Large interval motion

Let $t_1 < t_0$. Then, for $\omega(t_0 - t_1) >> 1$, $\mathcal{E}(\omega, t_1)$ is very small for $\beta_n < 1$. On the other hand, for $\beta_n > 1$,

$$\mathcal{E}(\omega, t_1) = \frac{2\omega t_1 e^2 \beta}{c}(1 - \frac{1}{\beta_n^2}). \qquad (3.26)$$

This coincides with the frequency distribution of the radiated energy during the whole charge motion in the Frank-Tamm theory.
Let now $t_1 > t_0$. Then, for $\omega t_0 >> 1$ (but $t_1 > t_0$), one gets

$$\mathcal{E}(\omega, t_1) \approx -\frac{2e^2}{\pi cn}[2 - \cos \omega(t_1 - t_0)](1 + \frac{1}{2\beta_n}\ln \frac{1-\beta_n}{1+\beta_n}) \qquad (3.27)$$

for $\beta_n < 1$ and

$$\mathcal{E}(\omega, t_1) \approx \frac{2e^2\beta}{\pi c}\{\pi\omega t_0(1 - \frac{1}{\beta_n^2})-$$

$$-\frac{1}{\beta_n}[2 - \cos \omega(t_1 - t_0)](1 + \frac{1}{2\beta_n}\ln \frac{1-\beta_n}{1+\beta_n}) - \frac{\pi}{2\beta_n^2}\sin \omega(t_1 - t_0)\} \qquad (3.28)$$

for $\beta_n > 1$.
Nonoscillating parts of these expessions coincide with Eqs. (2.5) given by Tamm. According to his own words, Eqs. (2.5)
"are obtained by neglecting the fast-oscillating terms of the form $\sin \omega t_0$"
Tamm gives only Eqs.(2.5) and (2.6) without deriving them). Since some terms in (3.23) and (3.24) depend on $(1 - \beta_n)(t_0 - t_1)$ and $(1 - \beta_n)(t_0 + t_1)$ parameters, Eqs.(3.26)-(3.28) are not valid for $\beta_n \sim 1$ (this corresponds to Cherenkov's threshold).

11

3.4.2 Frequency distribution on the Cherenkov threshold

Thus, the case $\beta_n = 1$ needs a special consideration. One obtains

$$\mathcal{E}(\omega, t_1) = -\frac{e^2}{\pi n c}[\ln \frac{t_0 - t_1}{t_0 + t_1} - ci(2\omega(t_0 - t_1)) + ci(2\omega(t_0 + t_1))] \qquad (3.29)$$

for $t_1 < t_0$. This expression tends to zero for t_1 fixed and $t_0 \to \infty$.
On the other hand, for $t_1 > t_0$

$$\mathcal{E}(\omega, t_1) = \frac{2e^2}{\pi n c}\{[1 - \frac{1}{2}\cos\omega(t_1 - t_0)][C + \ln(4\omega t_0) - ci(4\omega t_0)] -$$

$$-[1 - \cos\omega(t_1 - t_0)][1 - \frac{\sin(4\omega t_0)}{4\omega t_0}] + \sin\omega(t_1 - t_0)[\frac{1 - \cos(4\omega t_0)}{4\omega t_0} - \frac{\pi}{4} - \frac{1}{2}\sin(4\omega t_0)].\} \quad (3.30)$$

The nonoscillating part of this expession coincides with that given by Tamm:

$$\mathcal{E}_T = \frac{2e^2}{\pi n c}[C + \ln(4\omega t_0) - 1].$$

On the other hand, Eq.(3.25) obtained by Kobzev and Frank for $\beta_n = 1$ goes into

$$\mathcal{E}_{KF} = \frac{2e^2}{\pi n c}[C + \ln(4\omega t_0) - 1 - ci(4\omega t_0) + \frac{\sin(4\omega t_0)}{4\omega t_0}].$$

For $(t_1 - t_0)$ fixed and $t_0 \to \infty$, Eq.(3.30) is reduced to

$$\mathcal{E}(\omega, t_1) = \frac{2e^2}{\pi n c}\{[1 - \frac{1}{2}\cos\omega(t_1 - t_0)][C + \ln(4\omega t_0)] -$$

$$-1 + \cos\omega(t_1 - t_0) - \sin\omega(t_1 - t_0)[\frac{\pi}{4} + \frac{1}{2}\sin(4\omega t_0)]\}. \qquad (3.31)$$

The main result of Section 3 is that Schwinger's approach incorporates both Tamm-Frank and Tamm problems. Tamm-Frank's results are obtained when the observation time $2t_1$ is smaller than the charge motion time t_0 and $t_0 \to \infty$. In particular, there is no radiation in nondispersive medium when the charge velocity is smaller than the light velocity in medium. The radiated energy rises in direct proportion to the observation time t_1 for $\beta_n > 1$. Tamm's problem is obtained when $t_1 > t_0$ and t_0 (and, therefore, t_1) tends to ∞. The intensity oscillates around Tamm's value for $\beta_n < 1$ and rises in proportional to the time of charge motion t_0 for $\beta_n > 1$.

4 Exact electromagnetic fields in Tamm's problem

Tamm's energy flux (2.8) radiated during the whole charge motion into the solid angle $d\Omega$ in the frequency range $d\omega$ is widely used by experimentalists for identification of the Cherenkov radiation. The aim of this section is to compare (2.8) with the energy flux obtained by exact solution of Tamm's problem.
But at first, we elucidate which approximations were made during the transition from

the exact vector potential (2.1) to Tamm's formula (2.8):

1) Changing R by R_0 outside the exponent means that observation is made on the sphere with radius R_0 much larger than the motion interval z_0, i.e.:

$$R_0 >> z_0. \tag{4.1}$$

2) Tamm's field strengths (2.3) are valid only in the wave zone where

$$\omega R_0/c_n >> 1 \tag{4.2}$$

3) When changing R under the sign of exponent in (2.1) by $R_0 - z'\cos\theta$, it is implicitly assumed that the quadratic term in the expansion of R is small as compared to the linear one. Consider this more carefully. We expand R up to the second order:

$$R \approx R_0 - z'\cos\theta + \frac{z'^2}{2R_0}\sin^2\theta.$$

Under the sign of exponent in (2.1), the following terms appear

$$\frac{z'}{v} + \frac{1}{c_n}(R_0 - z'\cos\theta + \frac{z'^2}{2R_0}\sin^2\theta).$$

appear. We collect terms involving z'

$$\frac{z'}{c_n}[(\frac{1}{\beta_n} - \cos\theta) + \frac{z'}{2R_0}\sin^2\theta].$$

Taking for z' its maximal value z_0, we present the condition for the second term in the expansion of R to be small in the form

$$z_0 << 2R_0(\frac{1}{\beta_n} - \cos\theta)/\sin^2\theta. \tag{4.3}$$

It is seen that the right-hand side of this equation vanishes for $\cos\theta = 1/\beta_n$, i.e., at the angle where the Cherenkov radiation exists. Therefore, in this angular region the second-order terms may be important.

4) Under the sign of exponent in (2.1) the second-order term should be small compared with π, i.e., the inequality:

$$\frac{z'^2\omega\sin^2\theta}{2R_0c_n} << \pi \tag{4.4}$$

should be hold. Or, taking for θ and z' their maximal values ($\theta = \pi/2, \quad z' = z_0$), one gets

$$\frac{z_0^2\omega}{2R_0c_n} << \pi. \tag{4.5}$$

From (4.2) and (4.5) one finds the following restriction on ω

$$\frac{c_n}{R_0} << \omega << \frac{2\pi R_0 c_n}{z_0^2}. \tag{4.6}$$

13

In the λ language ($\omega = 2\pi c/\lambda$) this condition looks like

$$\frac{n z_0^2}{R_0} << \lambda << 2\pi n R_0. \tag{4.7}$$

Let $\lambda = 4 \cdot 10^{-5} cm$, (the middle of optical region), $n = 1.5$ (glass). For the typical value $R = 100 cm$, the r.h.s. of (4.7) inequality is fulfilled with a great accuracy. Then, l.h.s. of (4.7) gives $z_0 << 5 \cdot 10^{-2} cm$. On the other hand, z_0 should not be too small. In fact, for $k_n z_0 << 1$, Tamm's formula (2.8) is reduced to

$$\frac{d^2 \mathcal{E}}{d\omega d\Omega} \sim \frac{e^2 \sin^2 \theta \omega^2 t_0^2}{\pi^2 c n \beta_n^2},$$

i.e., the Cherenkov diffraction picture disappears. Therefore, the width interval $10^{-4} cm < z_0 < 10^{-2} cm$ turns out to be optimal for the validity of Tamm's formula and existence of the pronounced Cherenkov maximum in the treated case.

It should be noted that for gases, these restrictions are less restrictive than for solids and liquids. In fact, since for them $n \approx 1$, one gets

$$(\frac{1}{\beta_n} - \cos \theta)/ \sin^2 \theta \approx \frac{1 - \cos \theta}{\sin^2 \theta} = 1/2 \cos^2(\theta/2).$$

Since for gases the angular spectrum is confined to the $\theta \approx 0$ region, Eq.(4.3) is reduced to (4.1). The same is true for Eq. (4.4). As a result, for gases, Tamm's expression (2.8) for the radiated power works when Eqs. (4.1) and (4.2) are fulfilled.
Conditions (4.1)-(4.7) ensuing the validity of Tamm's expressions are spreaded over different sources. We collected them together to make easier the interpretation of numerical results given below.

The energy flux through the unit solid angle of sphere of the radius R_0 for the whole time of charge motion is given by

$$\frac{dW}{d\Omega} = \frac{c}{4\pi} R_0^2 \int_{-\infty}^{\infty} dt (\vec{E} \times \vec{H})_r \tag{4.8}$$

Expressing $\vec{E}$ and $\vec{H}$ through their Fourier transforms

$$\vec{E} = \int \exp(i\omega t) \vec{E}_\omega d\omega, \quad \vec{H} = \int \exp(i\omega t) \vec{H}_\omega d\omega$$

and integrating over t, one gets

$$\frac{dW}{d\Omega} = \frac{c R_0^2}{2} \int_{-\infty}^{\infty} (\vec{E}(\omega) \times \vec{H}(-\omega)) d\omega = \int_{0}^{\infty} S(\omega) d\omega, \tag{4.9}$$

where

$$S(\omega) = \frac{d^2 W}{d\omega d\Omega} = c R_0^2 [\vec{E}_\theta^{(r)}(\omega) \vec{H}_\phi^{(r)}(\omega) + \vec{E}_\theta^{(i)}(\omega) \vec{H}_\phi^{(i)}(\omega)]. \tag{4.10}$$

This quantity shows how the Fourier component of the energy radiated for the whole time of charge motion is distributed over the sphere S. It does not depend on time. The superscripts (r) and (i) mean the real and imaginary parts of E_θ and H_ϕ. Exact field strengths obtained by differentiation of the exact vector potential (2.1) are given by

$$H_\phi^{(r)} = \frac{ek_n z_0}{2\pi c R_0} \sin\theta \int \frac{G}{R^2} dz', \quad H_\phi^{(i)} = \frac{ek_n z_0}{2\pi c R_0} \sin\theta \int \frac{F}{R^2} dz',$$

$$E_\theta^{(r)} = \frac{ek_n^2 z_0}{2\pi\omega\epsilon R_0} \sin\theta \left(\int \frac{1 - z'\epsilon_0 \cos\theta}{R^3} F_1 dz' - \frac{2}{k_n R_0} \int \frac{F}{R^2} dz' \right),$$

$$E_\theta^{(i)} = \frac{ek_n^2 z_0}{2\pi\omega\epsilon R_0} \sin\theta \left(\int \frac{1 - z'\epsilon_0 \cos\theta}{R^3} G_1 dz' + \frac{2}{k_n R_0} \int \frac{G}{R^2} dz' \right), \qquad (4.11)$$

where

$$F = \cos\psi - \frac{1}{k_n R_0 R} \sin\psi, \quad G = \sin\psi + \frac{1}{k_n R_0 R} \cos\psi,$$

$$F_1 = \sin\psi + 3\frac{\cos\psi}{k_n R_0 R} - 3\frac{\sin\psi}{k_n^2 R_0^2 R^2}, \quad G_1 = \cos\psi - 3\frac{\sin\psi}{k_n R_0 R} - 3\frac{\cos\psi}{k_n^2 R_0^2 R^2},$$

$$\psi = k_n R_0 \left(\frac{z'\epsilon_0}{\beta_n} + R \right), \quad R = (1 - 2z'\epsilon_0 \cos\theta + \epsilon_0^2 z'^2)^{1/2}, \quad \epsilon_0 = z_0/R_0.$$

The z' integration in (4.10) is performed over the interval $(-1, 1)$. For $\epsilon_0 << 1$ and $k_n R_0 >> 1$, $S(\omega)$ given by (4.10) transforms into the Tamm formula (2.8):

$$S_T = \frac{e^2 \sin^2\theta}{\pi^2 nc} \left[\frac{\sin k_n z_0 (\cos\theta - 1/\beta_n)}{\cos\theta - 1/\beta_n} \right]^2. \qquad (4.12)$$

There are three geometric parameters of the length dimension entering into (4.11) and (4.12):
the motion interval $L = 2z_0$, the radius of the observation sphere R_0, and the vacuum wavelength $\lambda = 2\pi c/\omega$ related to the medium wavelength $\lambda_n = \lambda/n$. It is essential that these parameters enter into the energy flux and field strengths through dimensionless combinations

$$\epsilon_0 = \frac{z_0}{R_0} = \frac{L}{2R_0}, \quad k_n z_0 = \frac{\pi n L}{\lambda}, \quad k_n R_0 = \frac{2\pi n R_0}{\lambda} = \frac{k_n z_0}{\epsilon_0}.$$

Thus, if only λ changes, ϵ_0 remains the same, but $k_n z_0$ and $k_n R_0$ vary. The typical exact (4.10) and Tamm's (4.12) intensities for the fixed $\epsilon_0 = 0.1$ and different L/λ are shown in Figs. 5-8 in logarithmic and usual scales. For convenience, we made intensities to be dimensionless, dividing them by the factor e^2/c. All the subseguent figures refer to $n = 1.5$, $\beta_n = 1.2$. We see that Tamm's intensities are close to exact ones for small and moderate ratios L/λ (Fig.5). Their difference becomes essential for large L/λ (Figs. 6-8). These figures demonstrate that disagreement between Tamm's and exact intensities may be essential despite the fact that ϵ_0 is small ($\epsilon_0 = 0.1$), and $k_n R_0$ is large ($k_n R_0 \approx 5 \cdot 10^3$, 10^4 and $2 \cdot 10^4$ for Figs. 6, 7, and 8, resp.) The reason for this is due to the violation of (4.5). In fact, the l.h.s. of (4.5) equals approximately 20, 40 and 100 for the situations shown in Figs. 6, 7 and 8, resp.

Another degree of freedom is to change only R_0. In this case, L/λ remains the same, but ϵ_0 and $k_n R_0$ change. The typical intensities for $L/\lambda = 200$ and different ϵ_0 are shown in Figs. 7, 9, and 10. It is seen that disagreement between Tamm's intensity and the exact one sharply increases when z_0 approaches R_0 (as it should be).

The last possibility is to change only z_0. In the dimensionless variables language, the means that $k_n R_0$ remains the same, while $k_n z_0$ and ϵ_0 change in such a way that their ratio remains the same. Figures 7,11, and 12 demonstrate that disagreement between Tamm's and exact intensities increases with z_0.

Previously, the experimentally observed broadening of the Cherenkov angular spectrum was attributed to the energy loss of a charged particle during its motion in medium [17, 18]. However, Figs. 6-8, and 10-12 demonstrate that the above broadening may be well associated with the violation of conditions (4.1)-(4.7). To be more specific, we turn to Ref. [18] in which the angular distribution of the radiation ($\lambda \approx 4 \cdot 10^{-5} cm$) arising from passage of Au heavy ions ($\beta \approx 0.87$) through the LiF slab ($n \approx 1.39$) of width $0.5 cm$ was studied. Substituting these parameters into (4.5), we see that the l.h.s. of this equation coincides with π for the observation sphere radius $R_0 \approx 40$ m. Obviously, this value is unrealistic. Since the realistic R_0 is about $1 - 2m$, the strong violation of (4.5) takes place.

The moral of this section is that one should be very careful when applying Tamm's formula (2.8) to the analysis of experimental data. The validity of conditions (4.1)-(4.7) ensuring the validity of (2.8) should be verified. The exact energy flux (4.10) should be used if these conditions are violated.

5 Conclusion

Let us briefly summarize the main results obtained:

1. In the framework of Schwinger's approach, closed expressions are obtained for the frequency and angular distributions for the energy radiated by a point charge moving uniformly in medium in a finite space interval (Tamm's problem). They generalize the formulae given by Frank and Tamm and are reduced to them in particular cases.

2. Tamm's approximate formula describing the frequency-angular distribution of the radiated energy in Tamm's problem is compared with the exact one. Criteria for the validity of Tamm's formula are checked by numerical calculations.

16
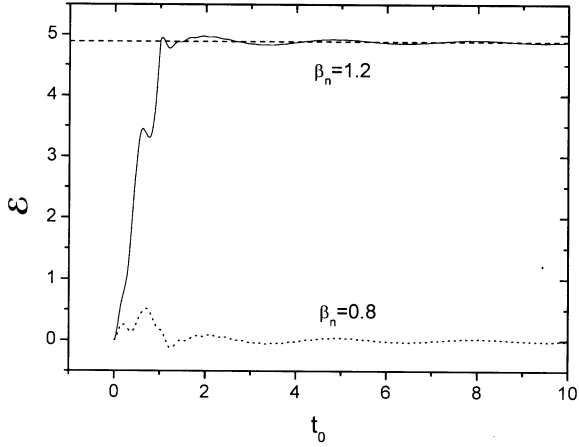
Figure 1: Energy $\mathcal{E}$ detected in a fixed time interval t_1 as a function of charge motion time t_0. For $\beta_n < 1$, $\mathcal{E}$ oscillates around zero. For $\beta_n > 1$ it oscillates around the finite value (3.25); $\mathcal{E}$ is given in units e^2/c, t_0 in units t_1.
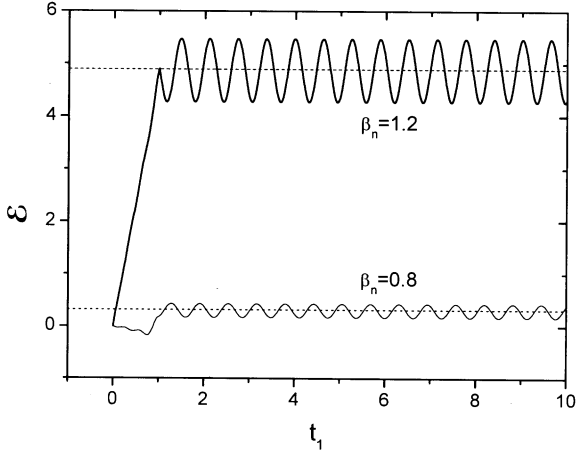

Figure 2: Energy $\mathcal{E}$ as a function of the detection time t_1. The time motion interval t_0 is fixed. For $\beta_n < 1$ and $\beta_n > 1$, $\mathcal{E}$ oscillates around the Tamm's values (2.5) and (2.6), resp. $\mathcal{E}$ is given in units e^2/c; t_1, in units t_0.

17
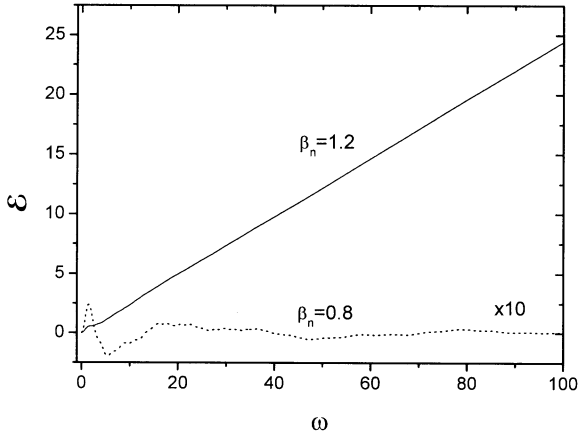
Figure 3: Frequency dependence of the radiated energy for $t_1/t_0 = 0.5$. $\mathcal{E}$ is given in units e^2/c; ω, in units $1/t_0$.
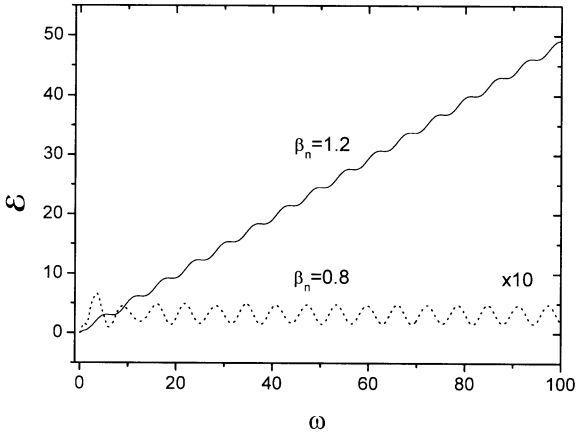
Figure 4: Frequency dependence of the radiated energy for $t_1/t_0 = 2$. $\mathcal{E}$ is given in units e^2/c; ω, in units $1/t_0$.

18
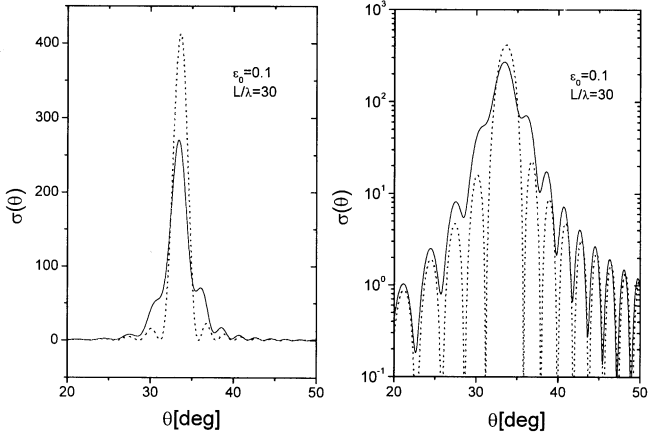
Figure 5: Exact (solid line) and Tamm's approximate (dotted line) angular dependences for $\epsilon_0 = z_0/R_0 = 0.1$, $L/\lambda = 30$, $\beta_n = 1.2$, $n = 1.5$. In Figs. 5-8, z_0 and R_0 are the same but λ changes.
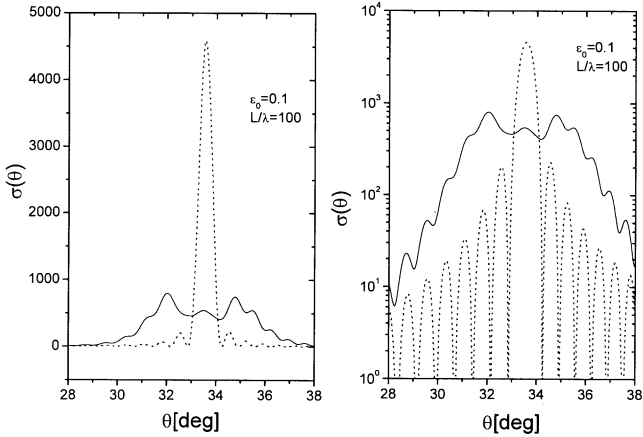
Figure 6: The same as in Fig.5, but for smaller λ corresponding to $L/\lambda = 100$. The deviation of the approximate curve from the exact one increases as λ diminishes.
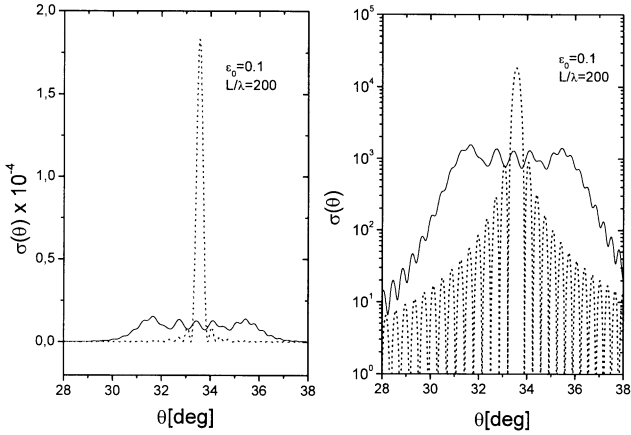
Figure 7: The same as in Fig.6, but for $L/\lambda = 200$.
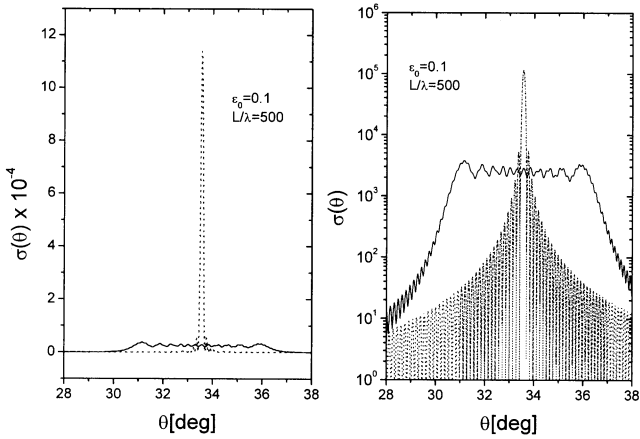
Figure 8: The same as in Fig.6, but for $L/\lambda = 500$.

20
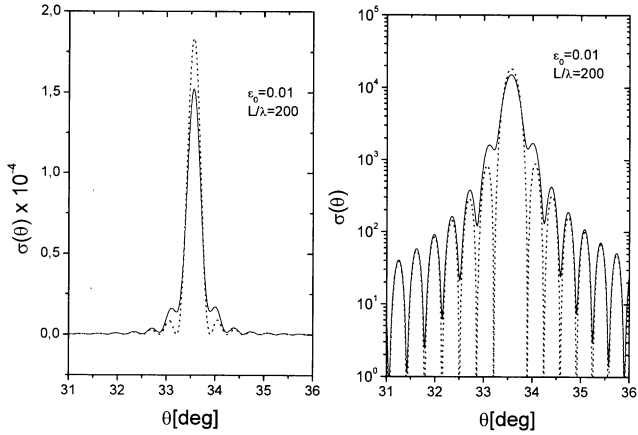
Figure 9: For small ϵ_0, the deviation of the approximate from exact curve is not very large. In Figs. 7, 9 and 10, L and λ are the same, but R_0 changes.
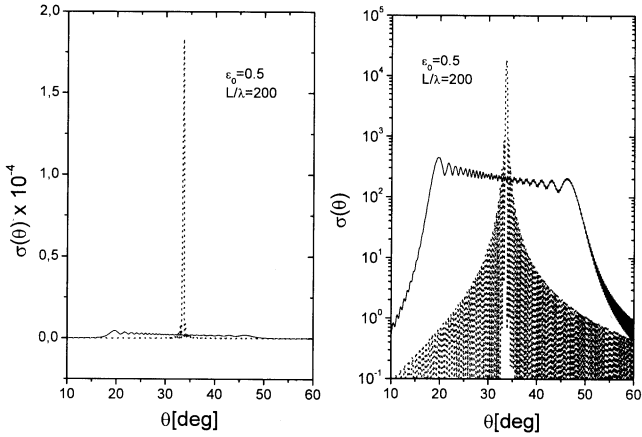

Figure 10: The same as in Fig. 9, but for smaller R_0 corresponding to $\epsilon_0 = 0.5$. The deviation of the approximate curve from the exact one is essential.

21
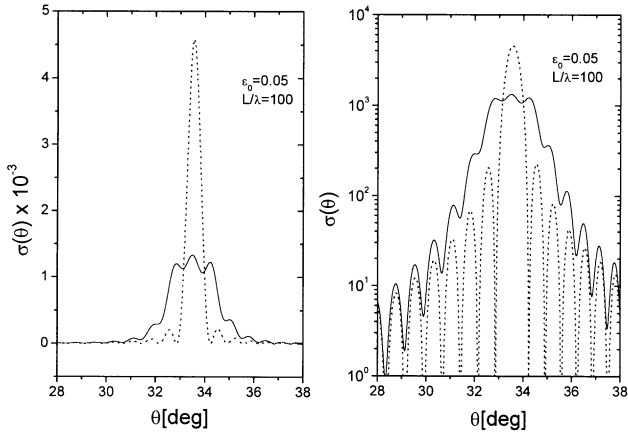
Figure 11: For small and moderate z_0 corresponding to $\epsilon = 0.05$, the deviation of the approximate curve from the exact one is not very essential. Figures. 7, 11 and 12 correspond to the same λ and R_0, but different z_0.
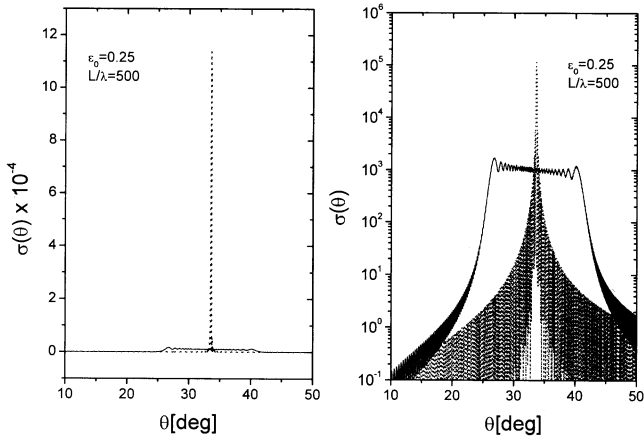

Figure 12: The same as in Fig. 11 but for larger z_0 corresponding to $\epsilon = 0.25$. The deviation of the approximate curve from the exact one becomes essential when z_0 approaches R_0.

References

[1] Tamm I.E., 1939, J.Phys. USSR, 1, 439.

[2] Lawson J.D., 1954, Phil. Mag., 45, 748.

[3] Lawson J.D., 1965, Amer. J.Phys., 33, 1002.

[4] Zrelov V.P. and Ruzicka J., 1989, Chech.J.Phys. B, 368-383.

[5] Zrelov V.P. and Ruzicka J., 1992, Chech.J.Phys., 42, 45-57.

[6] Afanasiev G.N., Beshtoev Kh. and Stepanovsky, 1996, Helv. Phys. Acta, 69, 111-129.

[7] Afanasiev G.N., Kartavenko V.G. and Stepanovsky Yu.P., 1999, J.Phys. D, 32, 2029.

[8] Schwinger J., 1949, Phys.Rev. A 75, 1912.

[9] Schwinger J. and Tsai W.Y., 1976, Ann. of Phys., 96, 303.

[10] Erber T., White D., Tsai W.Y. and Latal H.G., 1976, Ann. of Phys., 102, 405.

[11] Frank I.M., 1988, Vavilov-Cherenkov Radiation (Nauka, Moscow).

[12] Zrelov V.P., 1970, Vaviliov-Cherenkov Radiation in High Energy Physics (Israel Program for Scientific Translations, 1970)

[13] Aitken D.K. et al., 1963, Proc. Phys. Soc., 83, 710.

[14] Zrelov V.P. et al., 1983, Nucl. Instr. and Meth., 215, 141; 1988, Nucl. Instr. and Meth., A270, 62.

[15] Fano R.M., Chu L.J. and Adler R.B., 1960, Electromagnetic fields, energy and forces, (John Wiley, New York).

[16] Kobzev A.P. and Frank I.M., 1981, Yad. Fiz., 34, 125.

[17] Kuzmin E.S. and Tarasov A.V., 1993, Rapid Communications JINR, 4/61/-93, 64.

[18] Krupa L., Ruzicka J. and Zrelov V.P., 1995, JINR Preprint, P2-95-381.

Афанасьев Г.Н. и др.   Е2-2000-17
Швингеровский и точный подходы в задаче Тамма

Швингеровский подход позволяет по-новому взглянуть на задачу Тамма (покоящийся заряд мгновенно ускоряется, движется с постоянной скоростью, затем мгновенно замедляется). Швингеровские угловые и частотные распределения сравниваются с таммовскими, которые, в свою очередь, сравниваются с точными. Сформулированные условия справедливости известной формулы Тамма подтверждаются численными расчетами.

Afanasiev G.N. et al.   Е2-2000-17
Tamm's Problem in Schwinger's and Exact Approaches

Schwinger's approach gives a fresh look on Tamm's problem (charge, being initially at rest, exhibits an instant acceleration, moves with a finite velocity, and, after an instant deceleration, goes to the state of rest). Schwinger's angular and frequency distributions are compared with Tamm's ones, which in their turn are compared with exact distributions. Criteria for the validity of Tamm's formulae are checked by numerical calculations.

Макет Т.Е.Попеко